Bound and free atoms diagnosed by the recoil-induced resonances: One-dimensional optical lattice in a working magneto-optical trap

Maria Brzozowska, Tomasz M. Brzozowski, Jerzy Zachorowski, and Wojciech Gawlik*
Marian Smoluchowski Institute of Physics, Jagiellonian University, Reymonta 4, PL 30-059 Cracow, Poland†
(Received 31 October 2005; revised manuscript received 8 February 2006; published 29 June 2006)

We report on studies of simultaneous trapping of ^{85}Rb atoms in a magneto-optical trap (MOT) and one-dimensional optical lattice. Using Raman pump-probe spectroscopy, we observe the coexistence of two atomic fractions: the first consists of free, unbound atoms trapped in a MOT and the second is localized in the micropotentials of the optical lattice. We show that recoil-induced resonances allow not only temperature determination of the atomic cloud but, together with vibrational resonances, can also be used for real-time, nondestructive studies of the lattice loading and of the dynamics of systems comprising unbound and bound atomic fractions.

DOI: 10.1103/PhysRevA.73.063414 PACS number(s): 32.80.Pj, 42.50.Vk, 42.65.−k

I. INTRODUCTION

Optical lattices [1] constitute a convenient tool for studying phenomena related to periodically ordered systems. They are formed by the light-interference pattern, characterized by spatial, periodic light intensity and/or light polarization modulation. This modulation leads to a periodically varying dipole force which, acting on the sufficiently cold atoms, can lead to their localization in the minima or maxima of the light intensity distribution. Optical lattices with spatially modulated light polarization provide energy dissipation mechanisms resulting from cyclic optical pumping of the traveling atoms between their ground-state sublevels [2]. This leads to atom temperatures below the Doppler cooling limit [3]. Usually, optical lattices are filled with atoms either prepared in a magneto-optical trap (MOT) and further cooled in optical molasses or from the Bose-Einstein condensate [4]. In principle, lattice trapping can occur also in a MOT but this requires a special trapping beam configuration or complex phase stabilization schemes [5,6]. Investigation of optical lattices can be carried out by various methods. The most often used is the pump-probe Raman spectroscopy [7,8]. Others are based on observation of fluorescence from lattice-captured atoms [9] and transient recoil-induced intensity modulation of the Raman probe beam [10,11].

However, when the lattice trapping occurs in less than three dimensions or when the lattice potential is not sufficiently deep to capture all atoms, the atomic sample splits into two fractions, one moving freely and the other constrained, at least in one direction. Guo and Berman suggested to use recoil-induced resonances (RIRs) for studies of such systems [12] and analyzed theoretically various specific pump-probe configurations [12–15]. The first experiments employed one- and two-dimensional lattices loaded from optical molasses [7,8]. In these experiments, only the atoms captured by the lattice were interrogated and no information on unbound atoms was recorded. Still, as demonstrated in this paper, the ratio between free and bound atoms can be used as a convenient and sensitive indicator of the lattice dynamics and loading efficiency.

Below, we describe the method we have developed for the diagnostics of such two-fraction systems and present the results of our study. In our configuration, a one-dimensional (1D), blue-detuned, standing-wave optical lattice is created directly in a regular working MOT, i.e., with trapping fields constantly on. The configuration of the 1D lattice we apply is the simplest possible and imposes no polarization-gradient cooling. This leaves magneto-optical trapping as the only temperature-controlling mechanism that facilitates interpretation of the observations. We have verified that, indeed, the lattice beams do not change the atomic temperature, hence we can use them as Raman pumps for a nondestructive, 2D RIR thermometry [16]. By means of the Raman pump-probe spectroscopy, we study the interplay between two atomic fractions: one is too hot to be localized in the lattice micropotentials, and the other is captured by the lattice. To our knowledge, this is the first observation of a robust coexistence of an optical lattice with atoms trapped in a regular operating MOT.

The paper is organized as follows. In Sec. II, we briefly recall the principles of the Raman transitions between energy levels of a two-level atom, both for the case of a free, unbound particle as well as for an atom captured in a lattice micropotential. In Sec. III, we describe our experimental setup. In Sec. IV, the experimental results and their interpretation are given. Section V summarizes our work and indicates possible applications of our method.

II. RAMAN TRANSITIONS IN FREE AND BOUND ATOMS

We consider a two-level atom interacting with two counterpropagating laser beams of frequency ω and of the same linear polarization, as depicted in Fig. 1(a). Since the beams produce a standing-wave interference pattern, they act as lattice beams. A probe beam, of frequency $\omega+\delta$ and of the same polarization as the lattice beams, makes a small angle θ with one of the lattice beams. The probe beam detuning δ is scanned around zero and the probe absorption is monitored.

The probe and lattice beams drive Raman transitions with absorption of a photon from one beam followed by stimu-

*Electronic address: gawlik@uj.edu.pl
†URL: http://www.if.uj.edu.pl/ZF/qnog/

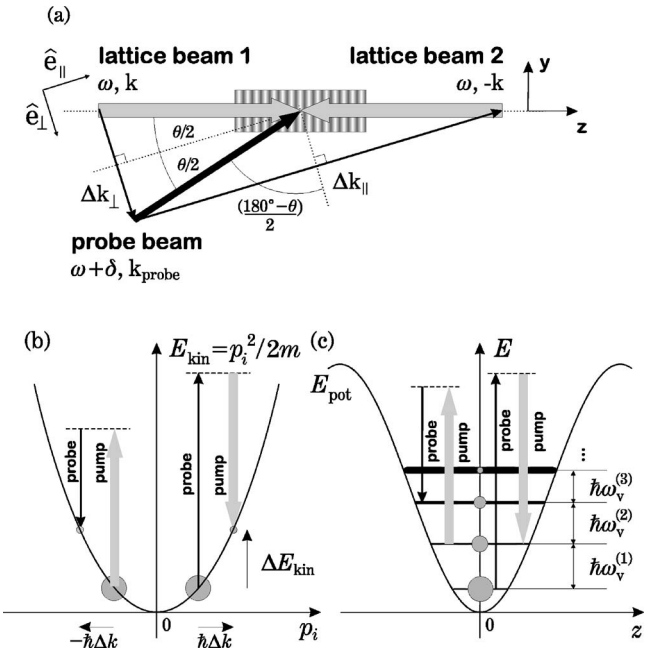

FIG. 1. (a) Geometry of the light beams and momentum transfers $\hbar\Delta\mathbf{k}_{\parallel}$ and $\hbar\Delta\mathbf{k}_{\perp}$ in the Raman transitions. (b) Raman transitions between kinetic states of free atoms. (c) Raman transitions between vibrational levels of atoms bound in the optical lattice potential. The vibrational level spacing decreases due to anharmonicity. In (b) and (c), circles symbolize populations of the relevant levels.

lated emission to the second beam [Fig. 1(b)]. Such processes couple two kinetic states of a free-moving atom. As a result, the atom gains kinetic energy $\Delta E_{\mathrm{kin}}=\hbar|\delta|$ and changes momentum $\mathbf{p}$ by $\Delta\mathbf{p}=\hbar\Delta\mathbf{k}=\pm 2\hbar k\hat{\mathbf{e}}_i \sin\alpha/2$. Here, k is the length of the light wave vector, α is the angle between the probe and either of the lattice beams: $\alpha=\theta$ for Raman transitions involving the nearly copropagating lattice beam, or $\alpha=180°-\theta$ for transitions involving the nearly counterpropagating lattice beam, whereas $\hat{\mathbf{e}}_i$ is the unit vector perpendicular to the bisector of α. The sign in $\Delta\mathbf{p}$ depends on the direction of the Raman process. The resulting net variation of the probe beam intensity, $s(\delta)$, depends on the population difference of the momentum states and shows a resonant behavior around $\delta=0$ [12–15,17,18]. This recoil-induced resonance has a shape of the derivative of the atomic kinetic momentum distribution along the momentum exchange direction, $s(\delta)\propto\partial\Pi(p_i)/\partial p_i$, where $p_i=\mathbf{p}\cdot\hat{\mathbf{e}}_i$.

Since two lattice beams combine with the probe to drive the Raman processes, two RIR signals are expected in the probe transmission spectrum. The width of the RIR signal, proportional to the width of the momentum distribution along relevant $\hat{\mathbf{e}}_i$, scales with the angle α as $\sin(\alpha/2)$. Hence, assuming that for given conditions the momentum distribution widths are of the same order, we expect one narrow contribution, resulting from recoil in the $\hat{\mathbf{e}}_{\perp}$ direction, and one wide contribution, associated with recoil in the $\hat{\mathbf{e}}_{\parallel}$ direction. The presence of the two well-resolved recoil signals in the recorded spectrum enables simultaneous determination of the momentum distributions in the two orthogonal directions [16]. When θ tends to zero, $\hat{\mathbf{e}}_{\parallel}$ ($\hat{\mathbf{e}}_{\perp}$) becomes parallel (perpendicular) to the z axis, which defines the direction of the optical lattice confinement.

The above mechanism works well for atoms that move freely along $\Delta\mathbf{k}$ and their kinetic energy can change in a continuous way. In our case, the motion of atoms confined in the 1D lattice wells becomes quantized in the z direction. This results in vibrational structure of energy levels, unevenly spaced by $\hbar\omega_v^{(1)}$, $\hbar\omega_v^{(2)}$, …, which differ because of anharmonicity of the potential [Fig. 1(c)]. By averaging the vibrational level spacing over anharmonicity with weights reflecting the temperature-dependent populations of given vibrational levels, one can find positions of the most distinct Raman vibrational resonances [7,20]. The first harmonic, $\delta=\pm\bar{\omega}_v^I$, and, overtone, $\delta=\pm\bar{\omega}_v^{II}$, are associated with the change of vibrational quantum numbers by 1 and 2, respectively. Atoms trapped in the lattice do not give rise to the wide RIR signal associated with movement in the $\hat{\mathbf{e}}_{\parallel}$ direction. They participate only in the generation of a narrow RIR and Raman vibrational spectrum. Such a suppression of recoil in an optical lattice, consistent with the previous predictions [12–15] and experiments [7,8], suggests a novel method for diagnostics of lattice loading by measuring the magnitude of the appropriate RIR signal.

Various kinds of pump-probe spectra discussed in this section are illustrated in Figs. 2(a) and 2(b), by the results of experiments described below in Sec. III. All measured signals are fitted with the formula

$$s(\delta)=-A_{\parallel}\frac{\partial\mathcal{G}(\delta,\xi_{\parallel})}{\partial\delta}-A_{\perp}\frac{\partial\mathcal{G}(\delta,\xi_{\perp})}{\partial\delta}+L_I[\mathcal{L}(\delta,-\bar{\omega}_v^I,\gamma^I)-\mathcal{L}(\delta,\bar{\omega}_v^I,\gamma^I)]+L_{II}[\mathcal{L}(\delta,-\bar{\omega}_v^{II},\gamma^{II})-\mathcal{L}(\delta,\bar{\omega}_v^{II},\gamma^{II})], \tag{1}$$

where $\mathcal{G}(\delta,\xi)$ is the normalized Gaussian describing kinetic momentum distribution of width ξ, and $\mathcal{L}(\delta,\omega,\gamma)$ is the Lorentzian used for modeling the Raman vibrational resonance of width γ centered at ω; $A_{\parallel}$ and $A_{\perp}$ represent amplitudes of the wide ($\parallel$) and narrow ($\perp$) RIR contributions, and L_I and L_{II} are the amplitudes of the vibrational resonances associated with the first harmonic at $\bar{\omega}_v^I$ and overtone at $\bar{\omega}_v^{II}$, respectively [22]. Figures 2(c) and 2(d) show isolated recoil and vibrational contributions of expression (1) to the spectrum of Fig. 2(b). In principle, in addition to the discussed RIR and vibrational transitions, elastic transitions with $\delta=0$ are possible both in an optical lattice and for free atoms. However, as shown in Refs. [12,14,15], the resulting Rayleigh elastic scattering contribution is negligibly small in our geometry and polarization configuration.

III. EXPERIMENT

In our experiment (see Fig. 3), we use the ^{85}Rb atoms trapped and cooled in a standard six-beam, vapor-loaded MOT [19]. Additional beams intersect at a small angle in the trap center: the lattice standing wave and the running probe beam. Both have the same, linear polarization and are blue-detuned from the trapping transition $5\,^2\boldsymbol{S}_{1/2}(F=3)-5\,^2\boldsymbol{P}_{3/2}(F'=4)$ by $\Delta_{\mathrm{latt}}=2\pi\times 140$ MHz$\approx 23.3\Gamma$, where Γ

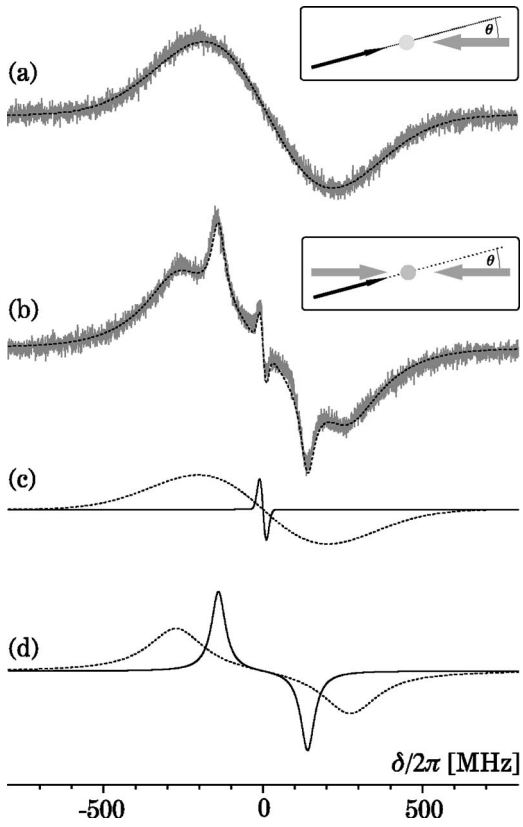

FIG. 2. Experimental spectra recorded at $T=64\ \mu$K and corresponding fits. (a) Single, wide RIR spectrum (gray) acquired in the simple two-beam configuration shown in the inset. Dotted black line represents the fit by the first term of Eq. (1). Such spectra are used to determine the temperature of the atomic cloud. (b) Experimental spectrum (gray) recorded in the presence of the 1D optical lattice (inset) and the fit by all terms of Eq. (1) (black). (c) RIR components of the fit: wide RIR associated with the momentum exchange in the $\parallel$ direction (dotted line) and narrow RIR associated with the exchange in the $\perp$ direction (solid line). (d) Vibrational components: first harmonic (solid line) and overtone (dotted line), extracted from the fit.

denotes the natural linewidth. The same polarization of the probe and lattice beams allows a multilevel structure of ^{85}Rb to be treated as a set of independent two-level systems. The relatively big detuning reduces resonant interaction with the atoms; the scattering rate did not exceed 44 kHz$\approx 7\times 10^{-3}\Gamma/2\pi$ for the lattice beam intensities $I_{\text{latt}}=5-35$ mW/cm^2. We have measured that such lattice intensities do not cause any visible heating. The trapping, probe, and lattice beams are generated by diode lasers injection-locked to a common, external-cavity master oscillator. The probe beam is scanned by $\delta/2\pi\approx\pm 1$ MHz around frequency ω of the lattice beam and its transmission is monitored by the photodiode.

IV. RESULTS

As already discussed in Sec. II, in our geometry of the probe and lattice beams, three contributions are expected in the probe transmission spectrum. Two of them are recoil-induced resonances: the narrow one involves the probe and the nearly copropagating lattice beam with $\Delta\mathbf{p}$ along the $\hat{\mathbf{e}}_\perp$ direction, and the wide one is for the probe and lattice beams nearly counterpropagating, with $\Delta\mathbf{p}$ along the $\hat{\mathbf{e}}_\parallel$ direction (Fig. 3). The third contribution is the vibrational spectrum resulting from Raman transitions between quantized energy levels of the atoms trapped and oscillating in the 1D lattice micropotentials [7]. The spectra acquired in our experiment indeed exhibit all expected contributions, as shown in Figs. 2(b)–2(d). It proves the coexistence of two atomic fractions in a MOT: the free moving atoms and the atoms captured by the 1D lattice. Thanks to the large detuning Δ_{latt}, resonances induced by the lattice and probe beams are not influenced by those involving the MOT beams. This is a significant simplification with respect to the previous work [21], allowing spectroscopic discerning of two stable atomic fractions and sensitive study of their coexistence.

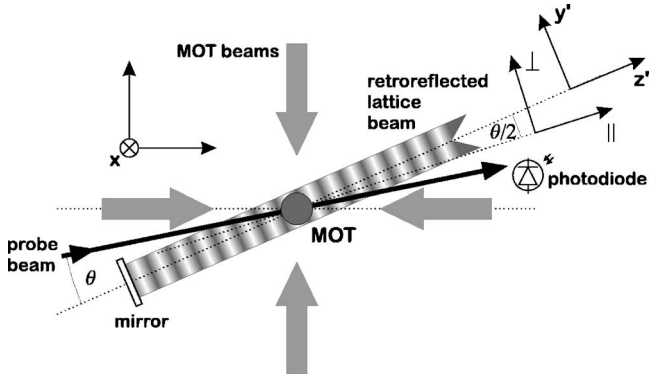

FIG. 3. Layout of the experiment. The pump and retroreflected lattice beams intersect in a cloud of cold atoms in the working MOT. The momentum exchange due to Raman transitions involving the probe and the lattice photons is allowed in two directions: $\perp$ and $\parallel$. The 1D lattice constrains atomic motion along the z direction, which, for small θ, nearly coincides with the $\parallel$ direction. The third pair of the MOT beams and the MOT coils is not shown.

Figure 4 presents the series of measurements taken for different temperatures of the atomic cloud. The temperature is controlled by the MOT beams intensity and is determined by the width of the wide RIR. At temperatures about the Doppler limit, $T_D=140\ \mu$K, atoms localized in lattice wells become a significant fraction of the whole sample and give rise to a pronounced vibrational structure.

In the spectra measured with the three-beam configuration, the first vibrational component is very distinct but the

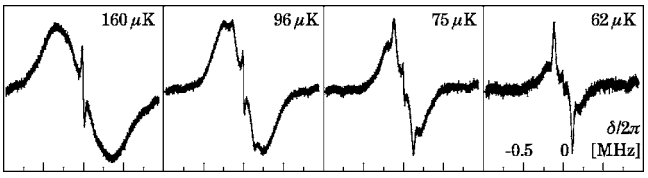

FIG. 4. Comparison of the probe transmission spectra for various MOT-beam temperatures. For sufficiently low temperatures, the wide RIR contribution disappears while the lattice contribution becomes distinct. The sequence of spectra illustrates well the competition between the free and bound atoms. Vertical scale is the same for all plots.

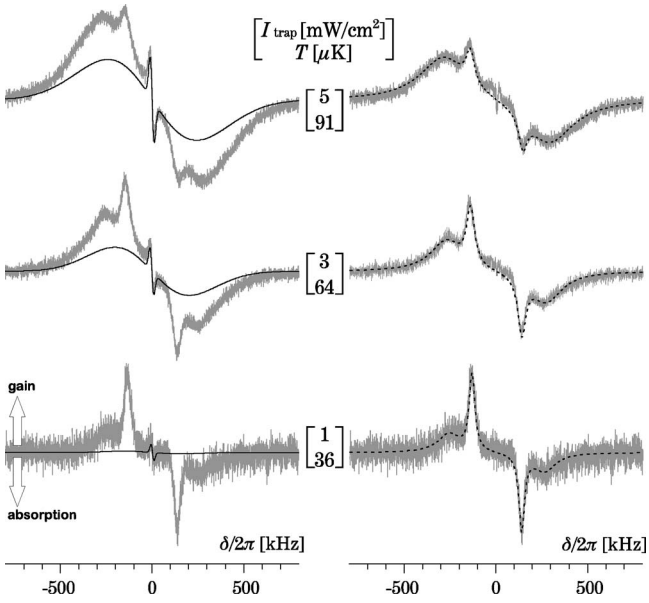

FIG. 5. Probe transmission spectra with 1D optical lattice recorded for various MOT-beam intensities and related temperatures. Left column, measured spectra (gray) and RIR contributions (solid black) determined from two-beam thermometry (see text). Right column, vibrational contributions extracted by substraction of RIR components from full spectra and theoretical fits (dotted). Vertical scale is the same for all plots.

overtone overlaps with the wide RIR, which greatly obstructs interpretation of the lattice spectra. This obstacle can be removed by a thorough separation of RIR and lattice contributions. For this reason, we reduced the number of free parameters by determining the temperature of the cold atomic cloud for each measurement. This was done by blocking the mirror that retroreflects the lattice beam (Fig. 3) and by performing two-beam RIR velocimetry with nearly counterpropagating Raman beams [16,23]. In such a configuration, the only contribution to the spectrum is the RIR associated with the momentum transfer along the $\hat{\mathbf{e}}_{\|}$ direction [Fig. 2(a)]. Since our blue 1D optical lattice does not exhibit spatial polarization modulation and operates on the $F \rightarrow F+1$ transition, no additional cooling mechanism is present [24]. This allows us to assume that the temperature of atoms in a MOT with and without the lattice is the same. Having determined the width $\xi_{\|}$, we calculated the temperature T and the width $\xi_{\perp} = \xi_{\|} \tan(\theta/2)$ [16,21]. Next, the widths $\xi_{\|}$ and $\xi_{\perp}$ were used as constants in the first terms of the fit given by Eq. (1), and then the fitted RIR contributions were subtracted from the spectra recorded with both lattice beams. The resulting difference constitutes pure lattice contribution, which is very well reproduced by the last terms of Eq. (1), as seen in Fig. 5.

For decreasing temperature of the atomic cloud, we observed an increase of the amplitude of the vibrational contribution relative to the RIR contribution. This indicates a growth of the fraction localized in the 1D optical lattice. We also observed systematic variation of the relative amplitudes of the two RIR contributions. As can be seen in Fig. 5, for lower temperatures the amplitude of the wide RIR associated with the momentum exchange in the $\|$ direction is noticeably smaller than the amplitude of the narrow RIR determined by the exchange in the $\perp$ direction. This behavior can be explained by constraints imposed by the 1D optical lattice on the atomic movement resulting in suppression of the recoil in the $\|$ direction. Hence, localized atoms do not contribute to the wide RIR. Since the increase of the lattice-trapped fraction caused by the temperature lowering proceeds at the expense of unbound atoms, the amplitude of the wide RIR becomes smaller. Inversely, since there is no lattice trapping in the $\perp$ direction, the localization does not affect the narrow RIR. In the considered range of temperatures, atoms populate practically all vibrational levels and localization is weak, therefore we can assume that the lattice-trapped and free atoms interact with the same average light intensity and ignore the fact that the bottoms of lattice potential wells coincide with the minima of light interference pattern. Consequently, we can assume that the narrow RIR signals associated with the two atomic fractions are generated with the same probability so that the net narrow RIR amplitude depends essentially on the total number of atoms. Further lowering of the temperature leads to the complete suppression of the wide RIR, which indicates that all atoms still remaining in a MOT are loaded into a 1D optical lattice. This qualitative consideration suggests the way to control the ratio of the lattice localized to unbound atoms.

To examine the behavior of the discussed atomic fractions quantitatively, we numerically estimated the number of atoms that give rise to the relevant terms of Eq. (1). Since RIR signals are proportional to the derivative of atomic momentum distributions, we first reconstructed their integrals and then evaluated the areas under resulting curves. In the case of lattice contributions, we calculated the areas directly under the vibrational Raman signals.

Figure 6(a) presents the area $S_{\text{narrow RIR}}$ as a function of MOT temperature. $S_{\text{narrow RIR}}$ is obtained by calculating the area under momentum distribution derived from the first term of Eq. (1) and dividing by the geometrical factor $\tan^2(\theta/2)$ [16,21] for comparison with $S_{\text{wide RIR}}$, the area associated with the second term of Eq. (1). Since there is no lattice trapping in this direction, $S_{\text{narrow RIR}}$ is proportional to the total number of atoms in the trap. In agreement with previous observations [25], it decreases linearly when the MOT-beam intensity is lowered.

Figure 6(b) depicts the ratio $(S_{\text{narrow RIR}} - S_{\text{wide RIR}})/S_{\text{narrow RIR}}$, which, due to the same transition amplitudes for both RIRs, is a direct measure of the fraction captured by the 1D optical lattice. As expected, the localized fraction grows with decreasing temperature. For a temperature of 30 μK, all the MOT-trapped atoms are in the optical lattice. The absolute number of atoms localized in the lattice also begins to grow with decreasing temperature, but then the general decrease of the total number of atoms in the MOT prevails. The number of atoms in the lattice reaches its maximum at about 60 μK when the captured fraction is close to 0.5.

For growing temperatures, we observed a systematic increase of the overtone contribution relative to the first

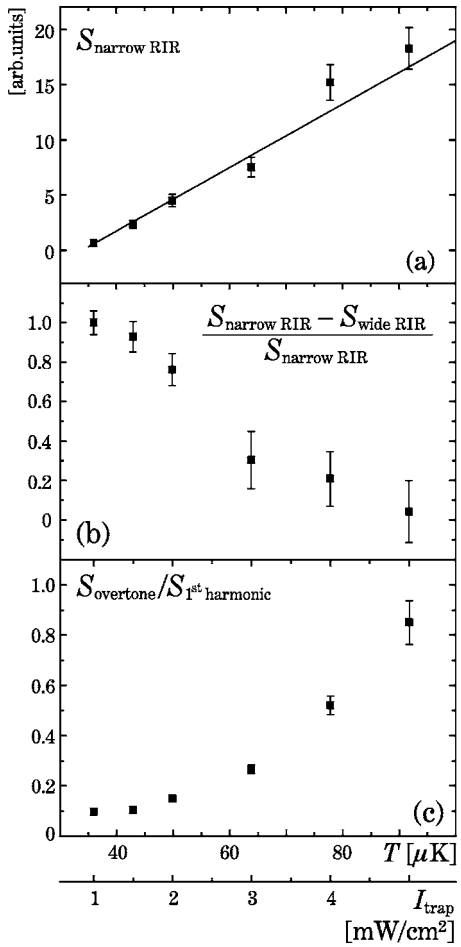

FIG. 6. Trap-beam intensity and temperature dependence of the atomic fractions estimated by calculating areas S associated with relevant spectra contributions: (a) $S_{\text{narrow RIR}}$, rescaled as described in the text, proportional to the total number of atoms in a MOT; (b) $(S_{\text{narrow RIR}}-S_{\text{wide RIR}})/S_{\text{narrow RIR}}$, the atomic fraction localized in a 1D optical lattice; (c) $S_{\text{overtone}}/S_{\text{first harmonic}}$, the ratio of atoms undergoing Raman transitions responsible for the overtone and first harmonic.

harmonic [$S_{\text{overtone}}/S_{\text{first harmonic}}$ ratio, depicted in Fig. 6(c)]. The rising probability of the overtone transitions is attributed to the fact that for higher temperature, population is shifted toward higher vibrational levels with more pronounced anharmonicity [26].

We have also studied changes of the position of the average first-harmonic frequency, $\bar{\omega}_v^I$, with the increase of the trapping-beam intensity, proportional to atomic temperature (Fig. 7). Taking only the temperature effect into account, one might expect a shift of the recorded vibrational resonances toward lower frequencies with the increasing temperature, since the higher vibrational levels become more populated. However, the observed dependence is opposite: $\bar{\omega}_v^I$ increases when the trapping light becomes more intense. We interpret this effect by including also the light-shift effect. The levels of the atoms in a MOT with the lattice beams switched on are perturbed by two fields: the red-detuned MOT field and the blue-detuned lattice field. When the intensity of the trapping light is increased, the related light shifts of the ground

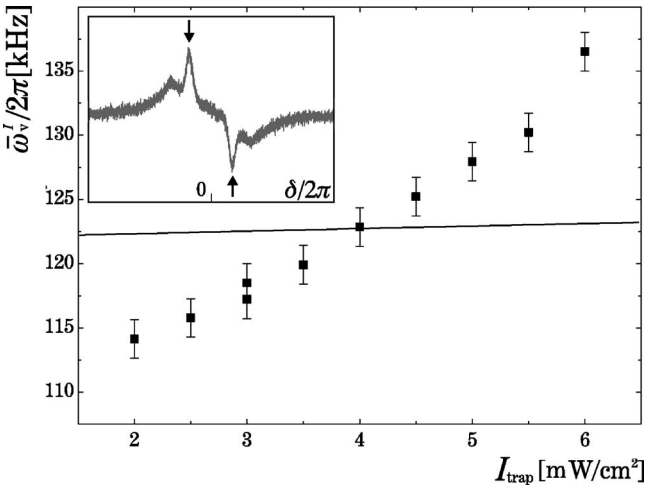

FIG. 7. Frequency $\bar{\omega}_v^I$ of the vibrational resonance (marked by arrows on the lattice spectrum in the inset) as a function of the MOT trapping beams intensity. The solid line represents predictions of independent light shifts, as described in the text.

atomic sublevels also increase. This decreases the detuning of the lattice beams from the atomic resonance frequency. Since the depth of the lattice potential U_{latt} is proportional to $I_{\text{latt}}/\Delta_{\text{latt}}$, we observe an increase of U_{latt} followed by an increase of $\bar{\omega}_v^I \propto \sqrt{U_{\text{latt}}}$. The calculations based on the assumption of independent light shifts associated with the MOT and lattice beams (solid line in Fig. 7), similar to those performed for far-detuned light [27], predict the correct slope, but fail to reproduce the size of the observed dependence of $\bar{\omega}_v$, which indicates a need for more refined calculations.

V. CONCLUSIONS

We have performed pump-probe spectroscopy of ^{85}Rb atoms in an operating MOT equipped with an extra pair of lattice beams, blue-detuned by more than 20Γ from the trapping transition $F=3-F'=4$. Application of a simple 1D lattice of a standing-wave configuration and nondestructive RIR thermometry allowed studies of the localization efficiency at well-determined atomic temperature, not affected by the lattice. The recorded pump-probe spectra revealed a complex structure composed of the recoil-induced and vibrational resonances due to the free and lattice-bound atoms, respectively. The magnitude of each of these spectral features yielded information on the population of the corresponding atomic fraction. We have shown how to resolve the pump-probe spectra for an atomic system consisting of two atomic fractions and applied this technique to the spectra taken at various atomic temperatures. This extension of a standard RIR velocimetry proved very useful for nondestructive diagnostics of 1D-lattice loading. We were able to verify that the creation of a robust 1D optical lattice is possible by loading of relatively hot ($\sim$100 μK) atoms directly from a continuously operating regular MOT without any further cooling.

ACKNOWLEDGMENTS

This work was supported by the Polish Ministry of Science and Information Society Technologies and is part of a general program on cold-atom physics of the National Laboratory of AMO Physics in Toruń, Poland. We would like to thank Julien Saby for his assistance in analysis of the experimental data, and Dmitry Budker and Krzysztof Sacha for their remarks on the manuscript.

[1] For a review, see, for example, G. Grynberg and C. Robilliard, Phys. Rep. **355**, 335 (2001), and references therein.
[2] J. Dalibard and C. Cohen-Tannoudji, J. Opt. Soc. Am. B **6**, 2023 (1998).
[3] P. D. Lett, R. N. Watts, C. I. Westbrook, W. D. Phillips, P. L. Gould, and H. J. Metcalf, Phys. Rev. Lett. **61**, 169 (1988).
[4] See, for example, M. Greiner, I. Bloch, O. Mandel, T. W. Hänsch, and T. Esslinger, Appl. Phys. B **73**, 769 (2001), and references therein.
[5] K. I. Petsas, A. B. Coates, and G. Grynberg, Phys. Rev. A **50**, 5173 (1994).
[6] H. Schadwinkel, U. Reiter, V. Gomer, and D. Meschede, Phys. Rev. A **61**, 013409 (1999).
[7] P. Verkerk, B. Lounis, C. Salomon, C. Cohen-Tannoudji, J.-Y. Courtois, and G. Grynberg, Phys. Rev. Lett. **68**, 3861 (1992).
[8] A. Hemmerich and T. W. Hänsch, Phys. Rev. Lett. **70**, 410 (1993).
[9] P. S. Jessen, C. Gerz, P. D. Lett, W. D. Phillips, S. L. Rolston, R. J. C. Spreeuw, and C. I. Westbrook, Phys. Rev. Lett. **69**, 49 (1992).
[10] M. Kozuma, Y. Imai, K. Nakagawa, and M. Ohtsu, Phys. Rev. A **52**, R3421 (1995).
[11] M. Kozuma, K. Nakagawa, W. Jhe, and M. Ohtsu, Phys. Rev. Lett. **76**, 2428 (1996).
[12] J. Guo and P. R. Berman, Phys. Rev. A **47**, 4128 (1993).
[13] J. Guo, P. R. Berman, B. Dubetsky, and G. Grynberg, Phys. Rev. A **46**, 1426 (1992).
[14] J. Guo, Phys. Rev. A **49**, 3934 (1994).
[15] J. Guo, Phys. Rev. A **52**, 1458 (1995).
[16] M. Brzozowska, T. M. Brzozowski, J. Zachorowski, and W. Gawlik, Phys. Rev. A **72**, 061401(R) (2005).
[17] J.-Y. Courtois, G. Grynberg, B. Lounis, and P. Verkerk, Phys. Rev. Lett. **72**, 3017 (1994).
[18] P. Verkerk, *Proceedings of the International School of Physics, Varenna, Course CXXXI* (IOS, Amsterdam, 1996), p. 325.
[19] E. L. Raab, M. Prentiss, A. Cable, S. Chu, and D. E. Pritchard, Phys. Rev. Lett. **59**, 2631 (1987).
[20] P. S. Jessen, C. Gerz, P. D. Lett, W. D. Phillips, S. L. Rolston, R. J. C. Spreeuw, and C. I. Westbrook, Phys. Rev. Lett. **69**, 49 (1992).
[21] T. M. Brzozowski, M. Brzozowska, J. Zachorowski, M. Zawada, and W. Gawlik, Phys. Rev. A **71**, 013401 (2005).
[22] Our calculations, based on C. Cohen-Tannoudji, J. Dupont-Roc, and G. Grynberg, *Atom-Photon Interactions: Basic Processes and Applications* (Wiley, New York, 1992), pp. 86–87 and 519–523, proved that higher overtones can be neglected.
[23] D. R. Meacher, D. Boiron, H. Metcalf, C. Salomon, and G. Grynberg, Phys. Rev. A **50**, R1992 (1994).
[24] D. Boiron, C. Triché, D. R. Meacher, P. Verkerk, and G. Grynberg, Phys. Rev. A **52**, R3425 (1995).
[25] See, for example, K. Lindquist, M. Stephens, and C. Wieman, Phys. Rev. A **46**, 4082 (1992).
[26] G. Herzberg, *Molecular Spectra and Molecular Structure* (Krieger, Malabar, FL, 1992), pp. 85–88.
[27] See, for example, T. Ido and H. Katori, Phys. Rev. Lett. **91**, 053001 (2003).